applied sciences

MDPI

Article

Research on Damage Mechanism and Performance-Based Design Process of Reinforced Concrete Column Members

Yukui Wang [1], Zhefeng Liu [2,*], Jia Guo [1] and Dou Zhong [1]

[1] School of Civil Engineering, Hunan City University, Yiyang 413000, China
[2] School of Civil Engineering, Changsha University of Science and Technology, Changsha 410114, China
* Correspondence: lzf0072006@163.com

Abstract: In order to understand the seismic damage assessment of reinforced concrete column members, the coupling relationship between the capacity degradation and the accumulated hysteretic energy and the displacement history was considered. The energy-based damage index under the random variable amplitude loading history was proposed. On the basis of preliminary research, the corresponding relationship between the damage index and the construction member parameters and seismic parameters was established, the damage mechanism was analyzed according to the damage index, and then the performance-based design process was proposed. It was found that increase in the stirrup ratio can slow down the damage, and the slowing effect was initially fast and then slows. When the reinforcement ratio is doubled, the damage index decreased by 0.063. The longer the earthquake duration was, the more serious the damage was, and this phenomenon was more obvious when the ductility coefficient was larger. With the increase in the ductility coefficient, the damage continuously increased. Therefore, it is an effective way to decrease the damage by controlling the ductility coefficient. Among all the influencing factors, the fundamental period and seismic intensity contributed more significantly to the damage indicators. When the damage index (performance objective) was determined, the target stirrup ratio can be obtained according to the proposed performance design process, that is, this design process can be used in the performance-based design. The design method based on damage index can make up for the deficiency that the design method based on the ductility coefficient does not consider the earthquake duration.

Keywords: reinforced concrete column; safety assessment; random variable; damage index; damage mechanism

Citation: Wang, Y.; Liu, Z.; Guo, J.; Zhong, D. Research on Damage Mechanism and Performance-Based Design Process of Reinforced Concrete Column Members. *Appl. Sci.* **2023**, *13*, 1452. https://doi.org/10.3390/app13031452

Academic Editor: Dario De Domenico

Received: 17 December 2022
Revised: 16 January 2023
Accepted: 17 January 2023
Published: 22 January 2023

1. Introduction

In the performance-based design process, the structural safety assessment targets should be quantified according to the damage index [1–3]. A reasonable damage index not only reflects the damage caused by the three elements of the earthquake (amplitude, frequency spectrum, and earthquake duration) [4–7], but also establishes a corresponding relationship with the construction member parameters to improve the mechanical properties of the structure [8]. The existing damage index can be classified into three aspects: (a) degradation-based damage index; (b) deformation-based damage index; and (c) energy-based damage index.

The degradation-based damage index describes structural damage by using the changes of structural characteristics, such as stiffness [9], frequency [10], and strength [11]. Although the degradation-based damage index does not directly include the three elements of the earthquake, it reflects the structural damage caused by the three elements. Therefore, the degradation-based damage index is applied to describe the structural damage. However, the deficiency of the degradation-based damage index is that it cannot establish a corresponding relationship with the construction member parameters. The deformation-based damage index considers that the structure damage is caused by the maximum displacement deformation; the ratio of the maximum displacement deformation to the limit displacement deformation is used to define the damage [12]. The deformation-based damage index takes the deformation demand as the design target, which can directly understand the deformation state of the structure under the earthquake actions, but the disadvantage is that the impact of earthquake duration has not been effectively considered.

There is a lack of correlation between the maximum displacement deformation of the structure and the earthquake duration [13], but there is a good correlation between the earthquake duration effect and the accumulated hysteretic energy of the structure under the earthquake actions [14]. With the intensification of the decay process, the correlation between the earthquake duration effect and the accumulated hysteretic energy is higher [15]. Therefore, the accumulated hysteretic energy is widely used to express the earthquake duration effect [16]. The energy-based damage index not only includes the construction member parameters, but also reflects the effect of the earthquake duration (accumulated hysteretic energy), which can comprehensively reflect the structural damage caused by the earthquake actions. Therefore, the energy-based damage index is the main research focus.

In 1985, the damage index with displacement deformation term and accumulated hysteretic energy term was established by Park and Ang [17,18]. This intuitive expression (a simplified linear relationship of displacement deformation term and accumulated hysteretic energy term) is easy to accept, and the Park–Ang damage index establishes a quantitative relationship with construction member parameters (yield load, reinforcement conditions, and ductility conditions), which makes it possible to reverse design based on damage targets. Therefore, this damage index has been used to describe damage by many scholars, but the simplification in form cannot truly reflect the damage mechanism. Despina and Jason et al. [19,20] found that the influence of ultimate deformation capacity of RC columns was mainly due to the plastic cumulative damage of longitudinal reinforcements and stirrups. Feng et al. [21] found that the ultimate deformation capacity was related to the accumulated hysteretic energy, while Liu et al. [15] found that the earlier the maximum displacement occurs during the loading process, the greater the accumulated hysteretic energy damage of the structure. It can be seen that there is a coupling relationship between the accumulated hysteretic energy term and the displacement deformation term. In order to maintain the simple linear relation of the Park–Ang damage index, the coupling relationship between the accumulated hysteretic energy term and the displacement deformation term is determined by the β factor. However, the solution of the β factor is not based on the analysis of the coupling relation. Therefore, the energy-based damage index needs to be further studied.

The capacity degradation of reinforced concrete column members was studied [15], and the energy-based damage index under random variable amplitude loading history was proposed [22]. On the basis of this preliminary research, in this study, the corresponding relationship between the damage index and the construction member parameters and the seismic parameters was established, and the damage mechanism was analyzed according to the damage index, and then the performance-based design process is proposed.

2. Energy-Based Damage Index

2.1. The Proposed Energy-Based Damage Index

The random variable amplitude loading history was applied to the reinforced concrete column members with different reinforcement levels, the causes of capability degradation were studied, and the energy-based damage index D_k was proposed [22], as follows:

$$D_k = \left[A_k\left(1 - \mathrm{e}^{-0.47 B_k n_k}\right)\right]^{0.09} \tag{1}$$

with

$$A_k = 0.62{\mu_\mathrm{e}}^{0.2} \tag{2}$$

$$B_k = \frac{3.64{\rho_\mathrm{sv}}^{-0.13}}{(1+\mu_\mathrm{e})^{5.63{\rho_\mathrm{sv}}^{0.09}}} \tag{3}$$

$$\mu_e = \frac{0.1H}{u_y} \tag{4}$$

$$n_k = \frac{E_C}{0.5F_y u_y} \tag{5}$$

where the parameter A_k is the peak value of damage index D_k, the parameter B_k is the energy dissipation requirements of the reinforced concrete column members, μ_e is the normalized amplitude, ρ_{sv} is the stirrup ratio of densification zone, H is the height of the member, n_k is the normalized accumulated hysteretic energy, E_C is the total energy dissipation, and F_y and u_y are the yield load and yield displacement, respectively.

According to Formulas (1)–(5)

$$D_k = f(H, \rho_{sv}, F_y, u_y, E_C) \tag{6}$$

It can be found from Formula (6) that the corresponding relationship between the damage index D_k and the construction member parameters (H, ρ_{sv}, F_y, u_y) and the total energy dissipation E_C is established.

2.2. Influence of Reinforcement Conditions and Total Energy Dissipation E_C on Damage Index D_k

When the section and height of the reinforced concrete column member are determined, the yield load F_y and the yield displacement u_y are related to the longitudinal reinforcement. Therefore, according to Formula (6), the influence of the stirrup ratio ρ_{sv}, the longitudinal reinforcement (F_y, u_y), and the total energy dissipation E_C on the damage index D_k is discussed.

Figure 1 shows the influence of the stirrup ratio ρ_{sv}, the longitudinal reinforcement conditions, and the total energy dissipation E_C on the damage index D_k, where the height of the column member H is 3000 mm. When the longitudinal reinforcement is relatively small ($\rho_{s,small}$), F_y and u_y are taken as 51.50 kN and 11.07 mm, respectively, and when the longitudinal reinforcement is relatively large ($\rho_{s,large}$), F_y and u_y are taken as 89.02 kN and 16.66 mm, respectively [13]. The x-coordinate is the stirrup ratio ρ_{sv}, and its range is 0.1% to 3%. The y-coordinate is the total energy dissipation E_C, and its range is 0 to 100,000 kN·mm. The z-coordinate is the damage index D_k, and its range is 0 to 1.

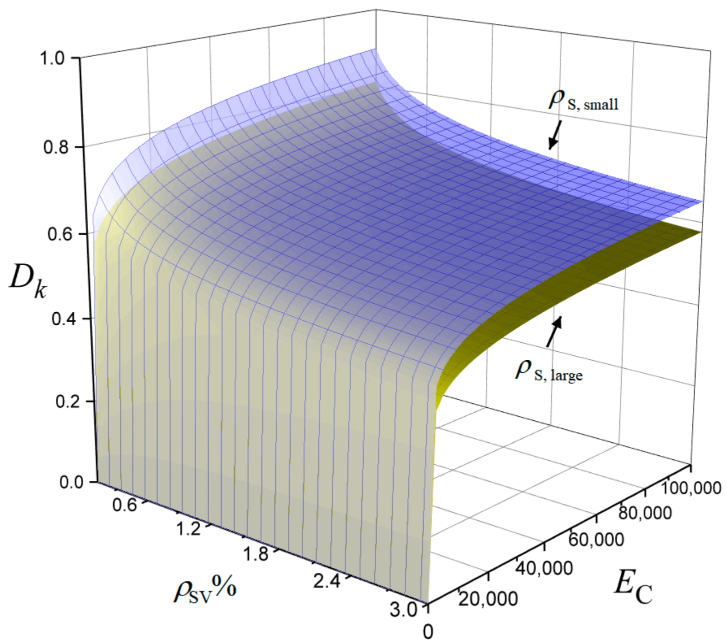

Figure 1. The influence of the stirrup ratio ρ_{sv}, the longitudinal reinforcement conditions, and the total energy dissipation E_C on the damage index D_k.

It can be found from Figure 1, with the increase in the total energy dissipation E_C, the damage index D_k increased monotonically from 0 to 1, that is, a one-to-one correspondence between the total energy dissipation E_C and the damage index D_k can be established. The increase in the stirrup ratio ρ_{sv} can slow down the damage development, and the slowing process is initially fast and then slows down. The increase in longitudinal reinforcement can significantly decrease the damage.

In order to further understand the quantitative description of the damage reduction value caused by the increase in the number of longitudinal reinforcement, the longitudinal reinforcement ratios of 0.587%, 0.971%, and 1.198% were used to study the quantitative relationship. According to Reference [15], when the longitudinal reinforcement ratio ρ_s is 0.587%, F_y and u_y are taken as 51.50 kN and 11.07 mm, respectively, when the reinforcement ratio ρ_s is 0.971%, F_y and u_y are taken as 80.11 kN and 14.39 mm, respectively, and when the reinforcement ratio ρ_s is 1.198%, F_y and u_y are taken as 89.02 kN and 16.66 mm, respectively. In order to ensure that the total energy dissipation and the maximum displacement amplitude experienced by the three specimens are the same, the total energy dissipation E_C was set as 100,000 kN·mm, and the nominal amplitude μ_e was set as 20. The stirrup ratio of the three specimens was set as 0.402%. The D_k–ρ_s relationship is shown in Figure 2 and is essentially linear. A linear formula that passes through the origin was used to fit the data, from which the Formula (7) can be obtained. According to Formula (7), in the proposed damage model, when the reinforcement ratio ρ_s increases by 10 times, the damage index decreased by 0.063.

$$D_k = 0.86 - 10.74\rho_s \tag{7}$$

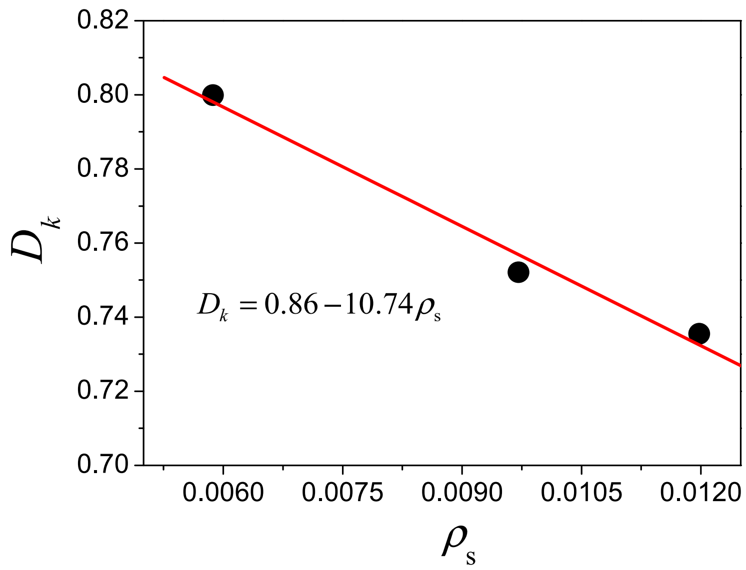

Figure 2. D_k–ρ_s relationship.

2.3. Solution Method of the Total Energy Dissipation E_C

In order to guide the seismic design, it is necessary to establish an effective relationship between the seismic design parameters and the energy-based damage index D_k. Therefore, the total energy dissipation E_C of the single degree-of-freedom structure was obtained by Kunnath [23] and Miao [24] as follows:

$$E_C = \frac{0.3455 m\eta E_s}{n} \tag{8}$$

with

$$\eta = 1.13\frac{(\mu - 1)^{0.82}}{\mu} \tag{9}$$

$$E_s = 0.5(\psi V_{PG})^2 \tag{10}$$

$$\psi = \begin{cases} \psi_v(\frac{2T}{T_g} - (\frac{T}{T_g})^2) & T < T_g \\ \psi_v(\frac{T}{T_g})^{-\gamma} & T > T_g \end{cases} \tag{11}$$

$$\psi_v = \frac{0.25A_{PG}}{V_{PG}}\sqrt{t_d T_g}\sqrt{\frac{\gamma + 0.5}{2\gamma + 2}} \tag{12}$$

$$T_g = 2\pi\frac{\tau_v V_{PG}}{\tau_a A_{PG}} \tag{13}$$

where m is mass of the structure, η is the ductility ratio parameters, E_s is the seismic energy per unit mass in elastic stage, n is the number of reinforced concrete column members, μ is the ductility coefficient, ψ is the displacement parameter for the input energy, ψ_v is the peak displacement parameter, T and T_g represent the fundamental period and the characteristic period, respectively, γ is the parameter of ground motion (γ = 0.5 for the parameter of ground motion was used in this paper [25]), t_d is the earthquake duration, and V_{PG} and A_{PG} represent the peak velocity of ground and the peak acceleration of ground, respectively. The parameter τ_v was set to 1.9, and the parameter τ_a was set to 2.4 [26].

According to Formulas (8)–(13), the total energy dissipation E_C of the single degree-of-freedom structure can be obtained.

$$E_C = h(\mu, m, n, T, A_{PG}, V_{PG}, t_d) \tag{14}$$

It can be found from Formula (14) that the relationship between the total energy dissipation E_C and the ductility coefficient μ, the number of reinforced concrete column members n, the fundamental period $T(m)$, the seismic intensity (A_{PG} and V_{PG}), and the earthquake duration t_d is established.

3. Damage Mechanism Analysis Based on Damage Index

Previous studies have shown that the damage index D_k increases monotonically from 0 to 1 with the increase in total energy dissipation E_C. Therefore, the total energy dissipation E_C can be used as a carrier to study the relationship between the damage index D_k and the ductility coefficient μ, the period $T(m)$, the seismic intensity (A_{PG} and V_{PG}), and the earthquake duration t_d.

Figure 3 shows the influence of the ductility coefficient μ, the period $T(m)$, the seismic intensity (A_{PG} and V_{PG}), and the earthquake duration t_d on the total energy dissipation E_C. The x-coordinate is the earthquake duration t_d, and its range is 0 to 30 s. The y-coordinate is the ductility factor μ, and its range is 1 to 5. The z-coordinate is the total energy dissipation E_C. The variation range of the fundamental period T is 0.1 s~0.7 s. The seismic intensity is divided into three levels: 6 degrees (0.05 g), 7 degrees (0.1 g), and 8 degrees (0.2 g).

As shown in Figure 3a, the total energy dissipation E_C increased with the extended earthquake duration t_d, and the larger the ductility coefficient μ, the faster the total energy dissipation E_C increased. With the increase in ductility factor μ, the total energy dissipation E_C increased continuously. Therefore, an effective way to decrease the damage is by controlling the ductility coefficient. The total energy dissipation E_C increased with the increase in the fundamental period T, and the greater the fundamental period T, the faster the total energy dissipation E_C increased. Similar phenomena can be seen in Figure 3b,c. Comparing Figure 3a–c, the higher the seismic intensity, the more the total energy dissipation E_C increased. Among all the influencing factors, the fundamental period T and seismic intensity contributed more significantly to the total energy dissipation E_C. Since the damage index D_k increased monotonically with the increase in the total energy dissipation E_C, the influence of the ductility coefficient μ, the period $T(m)$, the seismic intensity (A_{PG} and V_{PG}), and the earthquake duration t_d on the damage index D_k can be obtained.

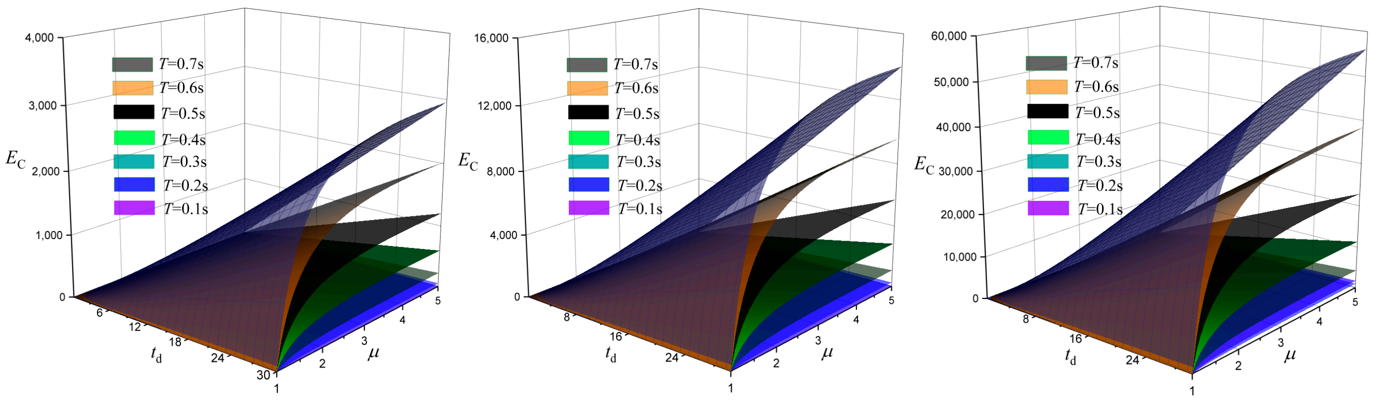

(**a**) (**b**) (**c**)

Figure 3. The influence of the ductility coefficient μ, the period $T(m)$, the seismic intensity (A_{PG} and V_{PG}) and the earthquake duration t_d on the total energy dissipation E_C: (**a**) 6 degrees (0.05 g); (**b**) 7 degrees (0.1 g); (**c**) 8 degrees (0.2 g).

Substitute Formula (14) into Formula (6)

$$D_k = f(H, \rho_{sv}, F_y, u_y, \mu, m, n, T, A_{PG}, V_{PG}, t_d) \quad (15)$$

In summary, the energy-based damage index D_k showed a corresponding relationship with the height H, stirrup ratio ρ_{sv}, longitudinal reinforcement (F_y, u_y), ductility coefficient μ, period $T(m)$, number of column members n, seismic intensity (A_{PG} and V_{PG}), and earthquake duration t_d. The increase in the stirrup ratio ρ_{sv} can slow down the damage, and the slowing process is initially fast and then slows. When the reinforcement ratio is doubled, the damage index decreased by 0.063. The longer the earthquake duration t_d is, the more serious the damage is, and this phenomenon is more obvious when the ductility coefficient μ is larger. With the increase in the ductility coefficient μ, the damage increased continuously. Therefore, an effective way to decrease the damage is by controlling the ductility coefficient. Among all the influencing factors, the fundamental period T and seismic intensity contributed more significantly to the damage indicators.

4. Performance-Based Design Process of Reinforced Concrete Column Members

4.1. Performance-Based Design Process

Based on the corresponding relationship between the energy-based damage index and the seismic parameters (A_{PG}, V_{PG}, and t_d) and the construction member parameters (H, ρ_{sv}, F_y, u, μ, m, n, T), the performance-based design process is proposed.

As shown in Figure 4, the seismic design method can be divided into the following five steps.

(1) Elastic design stage

The section of the reinforced concrete member was preliminarily selected. The modeling tool midas Gen was used to establish the single degree-of-freedom structure model, and the longitudinal reinforcement ratio of the target member under minor earthquakes was calculated by midas Gen. The structural fundamental period T was determined according to the stiffness and the mass of the structure.

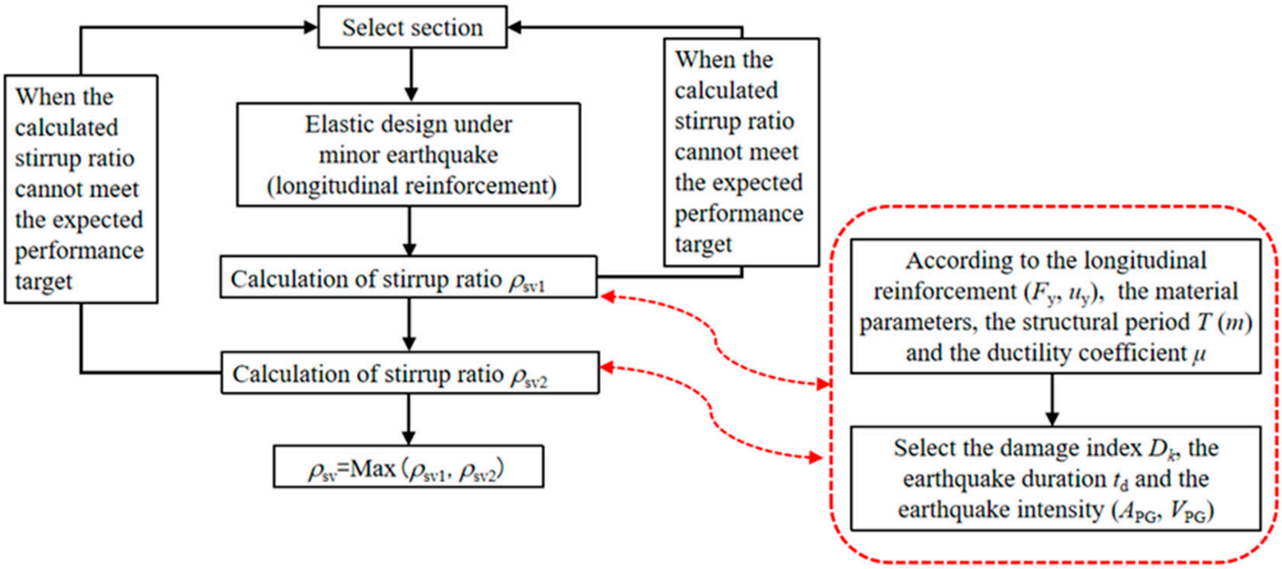

Figure 4. The performance-based design process.

(2) Calculation of the yield load

The yield displacement u_y of the target member can be obtained according to the pushover analysis. According to the yield displacement u_y, the material elastic modulus E and the dimensions, the yield load F_y can be obtained by Formula (16).

$$F_y = \frac{3EIu_y}{H^3} \tag{16}$$

Here, E is the material elastic modulus and I is the inertia moment of the section.

(3) Calculation of the ductility coefficient

The maximum displacement value u_{m1} under moderate earthquakes and the maximum displacement value u_{m2} under major earthquakes can be obtained according to the pushover analysis. Based on the maximum displacement value u_{m1} and yield displacement u_y, the ductility coefficient μ_1 under moderate earthquakes can be obtained by Formula (17). Similarly, the ductility coefficient μ_2 under major earthquakes can be obtained.

$$\mu = \frac{u_m}{u_y} \tag{17}$$

(4) Calculation of the stirrup ratio

By selecting the expected performance target (damage index D_k), the earthquake duration t_d and the seismic intensity (A_{PG} and V_{PG}), the stirrup ratio ρ_{sv1} under moderate earthquakes can be obtained according to Formula (15). When the calculated stirrup ratio cannot meet the expected performance target, the sectional dimensions and the longitudinal reinforcement need to be readjusted. Similarly, the stirrup ratio ρ_{sv2} under major earthquakes can be obtained.

(5) Determination of the stirrup ratio

By comparing the stirrup ratio ρ_{sv1} under moderate earthquakes and the stirrup ratio ρ_{sv2} under major earthquakes, the larger one is set as the final stirrup ratio ρ_{sv}.

4.2. Example

The performance-based design process is presented by using a single degree-of-freedom structure. When the seismic intensity was set to 7 degrees (0.1 g), the peak acceleration of ground A_{PG} under moderate earthquakes was 98 cm/s^2, and the peak acceleration of ground A_{PG} under major earthquakes was 220 cm/s^2. When the seismic intensity was set to 8 degrees (0.2 g), the peak acceleration of ground A_{PG} under moderate earthquakes was 196 cm/s^2, and the peak acceleration of ground A_{PG} under major earthquakes was 400 cm/s^2 [27]. The ratio of the peak velocity of ground V_{PG} to the peak acceleration of ground A_{PG} was 0.15 s [28].

In the example, the fundamental period T was changed by changing the floor load; the floor loads 40 kN/m^2, 60 kN/m^2, 80 kN/m^2, 100 kN/m^2, 120 kN/m^2, and 150 kN/m^2 were applied. The earthquake durations were set as 5 s, 10 s, 20 s, and 30 s [28]. Figure 5 shows the single degree-of-freedom structure. Table 1 is the design information for the structure. Table 2 contains the calculation results of the design parameters.

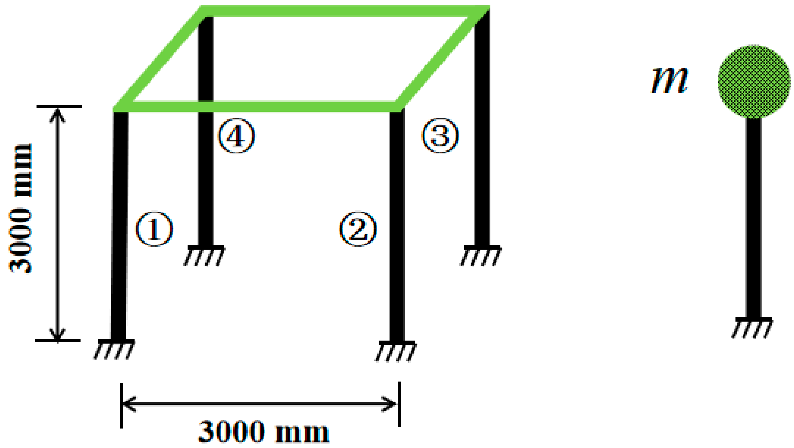

Figure 5. The single degree-of-freedom structure.

Table 1. The design information for the structure.

Member Type	Section Size $b \times h$ (mm × mm)	Height of Column H/ Length of Beam L (mm)	Strength Grade of Concrete	Longitudinal Reinforcement Type	Stirrup Type
Column Beam	400 × 400 200 × 350	3000 3000	C30	HRB335	HPB300

Table 2. The calculation results of the design parameters.

	Earthquakes	T (s)	M (kg)	μ	A_{PG} (cm/s^2)	V_{PG} (cm/s)	u_y (mm)	F_y (kN)
7 degrees (0.1 g)	Moderate earthquakes Major earthquakes	0.32	18,662	1.46	98 220	14.7 33	3	21.33
	Moderate earthquakes Major earthquakes	0.39	26,820.25	1.02	98 220	14.7 33	6	42.67
	Moderate earthquakes Major earthquakes	0.44	34,978.5	1.09	98 220	14.7 33	6	42.67
	Moderate earthquakes Major earthquakes	0.49	43,136.75	1.22	98 220	14.7 33	6	42.67
	Moderate earthquakes Major earthquakes	0.54	51,295.25	1.25	98 220	14.7 33	6	42.67
	Moderate earthquakes Major earthquakes	0.6	62,533.5	1.38	98 220	14.7 33	6	42.67

Table 2. *Cont.*

	Earthquakes	T (s)	M (kg)	μ	A_{PG} (cm/s^2)	V_{PG} (cm/s)	u_y (mm)	F_y (kN)
8 degrees (0.2 g)	Moderate earthquakes	0.32	18,662	1.43	196	29.4	6	42.67
	Major earthquakes				400	60		
	Moderate earthquakes	0.39	26,820.25	1.26	196	29.4	9	64
	Major earthquakes				400	60		
	Moderate earthquakes	0.44	34,978.5	1.36	196	29.4	9	64
	Major earthquakes				400	60		
	Moderate earthquakes	0.49	43,136.75	1.46	196	29.4	9	64
	Major earthquakes				400	60		
	Moderate earthquakes	0.54	51,295.25	1.21	196	29.4	12	85.33
	Major earthquakes				400	60		
	Moderate earthquakes	0.6	62,533.5	1.42	196	29.4	12	85.33
	Major earthquakes				400	60		

It can be found from Reference [22] that when the damage index is greater than 0.8, the column member is in the collapse state. When the damage index is less than 0.3, the column member is in the nondamaged state. Therefore, the change of the stirrup ratio is discussed when the damage index is 0.4, 0.5, 0.6, and 0.7. Since the design information of the column members are the same, this study only introduces the reinforcement results of column ①. The calculation results of the stirrup ratio are shown in Figure 6.

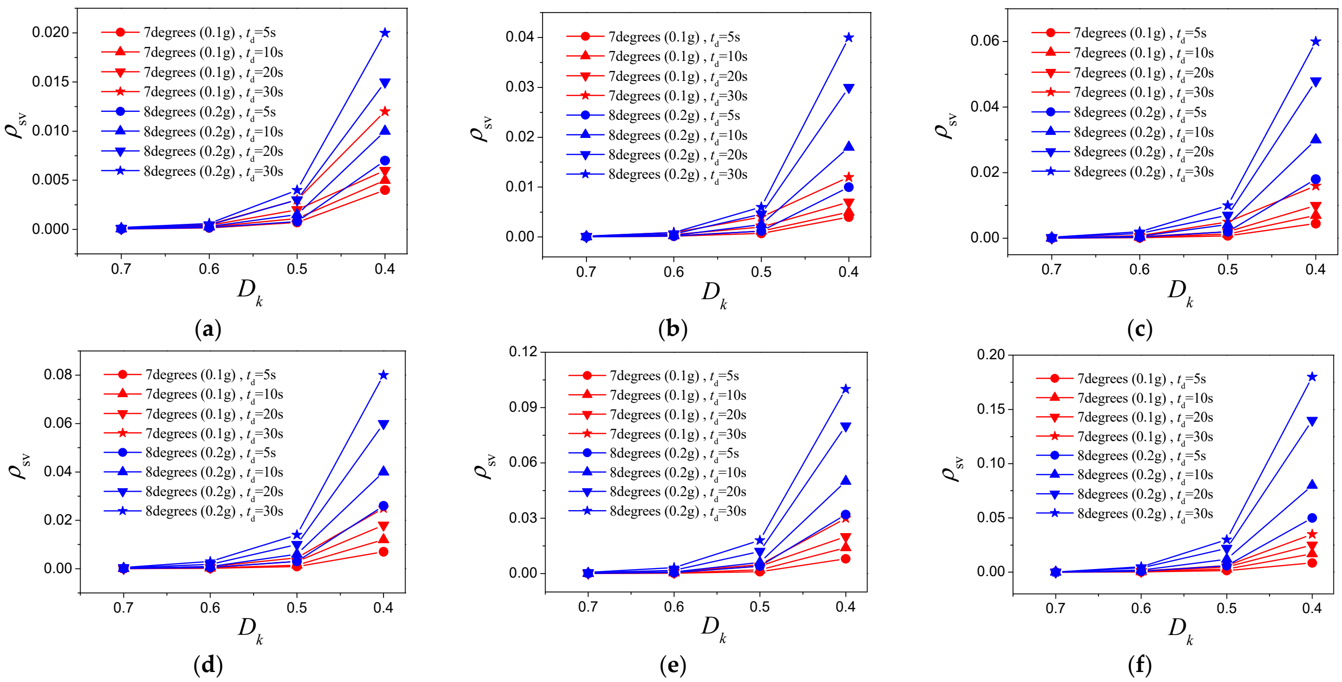

Figure 6. Calculation results of stirrup ratio at 7 degrees (0.1 g) and 8 degrees (0.2 g): (**a**) T = 0.32 s; (**b**) T = 0.39 s; (**c**) T = 0.44 s; (**d**) T = 0.49 s; (**e**) T = 0.54 s; (**f**) T = 0.6 s.

As shown in Figure 6a, when the earthquake duration t_d and earthquake intensity are constant, the increase in the stirrup ratio ρ_{sv} can slow down the damage. When the damage index D_k and seismic intensity are constant, the stirrup ratio ρ_{sv} increased with the increase in earthquake duration t_d, which indicates that the increase in earthquake duration t_d can aggravate the damage development of the construction member. When the earthquake duration t_d and damage index D_k are constant, the higher the seismic intensity, the greater the damage of the construction member. Similar phenomena can be seen in Figure 6b–f. Comparing Figure 6a–f, when the damage index D_k, the earthquake intensity, and the earthquake duration t_d are constant, the larger the fundamental period T is and the higher the stirrup ratio is, which indicates that the damage will be aggravated with an increase in the fundamental period T. It can be seen from Figure 6 that when the seismic intensity and earthquake duration t_d are constant, a one-to-one correspondence between the damage index D_k and the stirrup ratio ρ_{sv} was established. Therefore, when the damage index (performance objective) is determined by the owner, the target stirrup ratio can be obtained according to Figure 6, that is, this design process can be used in the performance-based design.

4.3. Comparison between the Design Method Based on Damage Index and the Design Method Based on Ductility Coefficient

Based on the code for seismic design of buildings [27], when the ductility coefficient $\mu \leq 1$, the construction member can be calculated according to linear elasticity, and there is no residual deformation after the earthquake. When the ductility coefficient $1 < \mu \leq 1.5$, the construction member is slightly damaged after the earthquake and can be used again after repair. When the ductility coefficient $1.5 < \mu \leq 2$, the construction member has medium damage after the earthquake and can be properly used after taking safety reinforcement measures. When the ductility coefficient $2 < \mu \leq 5$, the construction member is nearly severely damaged after the earthquake and can be used after major repair. When the ductility coefficient $\mu > 5$, the construction member is destroyed after the earthquake. Table 3 shows the performance index limit of the damage index-based design method and ductility coefficient-based design method [29].

Table 3. The performance index limit of damage index-based design method and ductility coefficient-based design method.

	Intact	Mild Damage	Moderate Damage	Severe Damage	Destruction
Performance index limit of damage index	$0 < D_k \leq 0.3$	$0.3 < D_k \leq 0.6$	$0.6 < D_k \leq 0.7$	$0.7 < D_k \leq 0.8$	$D_k > 0.8$
Performance index limit of ductility coefficient	$\mu \leq 1$	$1 < \mu \leq 1.5$	$1.5 < \mu \leq 2$	$2 < \mu \leq 5$	$\mu > 5$

In order to further study the difference between the design method based on the damage index versus the design method based on the ductility coefficient, according to the example (T = 0.49, 8 degrees), the D_k–ρ_{sv}–t_d relationship under different ductility coefficients is presented in Figure 7. The x-coordinate is the stirrup ratio ρ_{sv}, and its range is 0.1% to 3%. The y-coordinate is the earthquake duration t_d, and its range is 0 to 40. The z-coordinate is the damage index D_k, and its range is 0 to 1. When the limit value of ductility coefficient μ is 1.5, it means that the construction member designed according to the design method based on the ductility coefficient can ensure mild damage after an earthquake. When the limit value of the ductility coefficient μ is 2, it means that the construction member designed according to the design method based on the ductility coefficient can ensure moderate damage after an earthquake. When the limit value of the ductility coefficient μ is 5, it means that the construction member designed according to the design method based on ductility coefficient can ensure severe damage after an earthquake.

As shown in Figure 7a, the increase in stirrup ratio ρ_{sv} can slow down the damage development, and the slowing process is initially fast and then slows. With the increase in earthquake duration t_d, the damage index exceeded 0.6 (the performance index limit of mild damage). It can be seen that with the increase in earthquake duration t_d, the design method based on the ductility coefficient cannot meet the expected damage state of the construction member. However, the design method based on the damage index can make up for the deficiency where the design method based on the ductility coefficient does not consider the earthquake duration. Similar phenomena can be seen in Figure 7b,c.

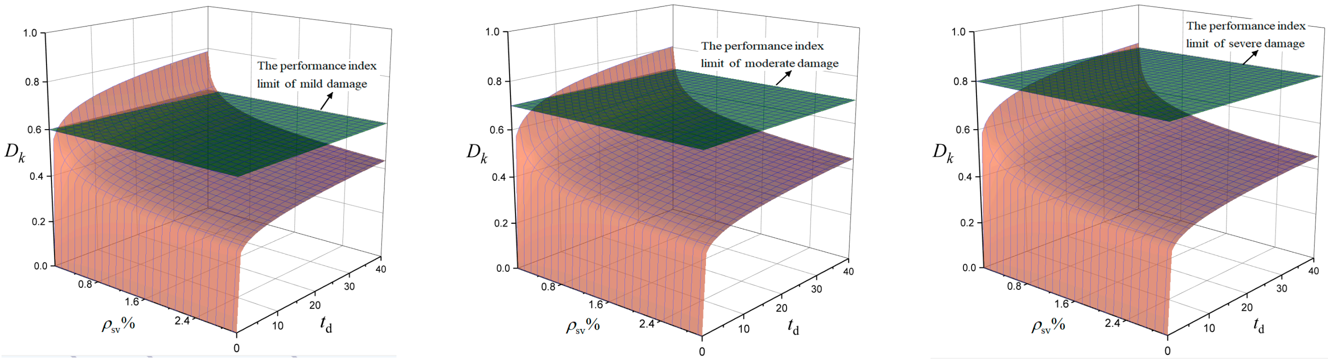

(a) (b) (c)

Figure 7. The D_k–ρ_{sv}–t_d relationship under different ductility coefficients: (**a**) μ = 1.5; (**b**) μ = 2; (**c**) μ = 5.

5. Conclusions

This performance-based design process was confined to reinforced concrete column members for the single degree-of-freedom structure, which can provide a basis for the study of performance-based design methods for multiple degree-of-freedom structures. The main conclusions and suggestions are as follows:

1. The corresponding relationship between the damage index and construction member parameters and seismic parameters was established.
2. The increase in stirrup ratio can slow down the damage, and the slowing effect was initially fast and then slow. When the reinforcement is doubled, the damage index decreased by 0.063.
3. The longer the earthquake duration was, the more serious the damage was, and this phenomenon was more obvious when the ductility coefficient was larger. With the increase in the ductility coefficient, the damage increased continuously. Therefore, an effective way to decrease the damage is by controlling the ductility coefficient. Among all the influencing factors, the fundamental period and seismic intensity contributed more significantly to the damage indicators.
4. This design process can be used in the performance-based design of reinforced concrete column members.
5. The design method based on the damage index can make up for the deficiency where the design method based on the ductility coefficient does not consider the earthquake duration.

Author Contributions: Conceptualization, Y.W. and Z.L.; methodology, J.G.; software, J.G.; validation, Y.W., J.G., and D.Z.; formal analysis, Y.W.; investigation, Y.W.; resources, Z.L.; data curation, D.Z.; writing—original draft preparation, Z.L.; writing—review and editing, Y.W.; visualization, Y.W.; supervision, J.G.; project administration, Z.L.; funding acquisition, Y.W. All authors have read and agreed to the published version of the manuscript.

Funding: This research was funded by the National Natural Science Foundation of China, grant number 50908022; the Natural Science Foundation of Hunan Province, grant number 2022JJ40023; and the Hunan University Students Innovation and Entrepreneurship Training Program Project, grant number S202211527024.

Data Availability Statement: The data presented in this study are available on request from the corresponding author.

Conflicts of Interest: The authors declare no conflict of interest.

References

1. Zhang, Z.; Liang, G.; Niu, Q.; Wang, F.; Chen, J.; Zhao, B.; Ke, L. A Wiener degradation process with drift-based approach of determining target reliability index of concrete structures. *Qual. Reliab. Eng. Int.* **2022**, *38*, 3710–3725. [CrossRef]
2. Zhong, K.; Lin, T.; Deierlein, G.G.; Graves, R.W.; Silva, F.; Luco, N. Tall building performance-based seismic design using SCEC broadband platform site-specific ground motion simulations. *Earthq. Eng. Struct. Dyn.* **2020**, *50*, 81–98. [CrossRef]
3. Xie, L.; Sha, H.; Chong, X.; Hou, L.; Guo, Y. Performance-based seismic design of RC frame structure with energy dissipative cladding panel connection system using equivalent energy design procedure. *J. Build. Eng.* **2022**, *59*, 105076. [CrossRef]
4. Jafari, M.; Pan, Y.; Shahnewaz, M.; Tannert, T. Effects of Ground Motion Duration on the Seismic Performance of a Two-Storey Balloon-Type CLT Building. *Buildings* **2022**, *12*, 1022. [CrossRef]
5. Zhang, Z.; Liu, X.; Zhang, Y.; Zhou, M.; Chen, J. Time interval of multiple crossings of the Wiener process and a fixed threshold in engineering. *Mech. Syst. Signal Process* **2020**, *135*, 106389. [CrossRef]
6. Hwang, S.H.; Mangalathu, S.; Jeon, J.S. Quantifying the effects of long-duration earthquake ground motions on the financial losses of steel moment resisting frame buildings of varying design risk category. *Earthq. Eng. Struct. Dyn.* **2021**, *50*, 1451–1468. [CrossRef]
7. Wang, W.; Li, D.-Q.; Liu, Y.; Du, W. Influence of ground motion duration on the seismic performance of earth slopes based on numerical analysis. *Soil Dyn. Earthq. Eng.* **2021**, *143*, 106595. [CrossRef]
8. Taghipoor, H.; Sadeghian, A. Experimental investigation of single and hybrid-fiber reinforced concrete under drop weight test. *Structures* **2022**, *43*, 1073–1083. [CrossRef]
9. Carrillo, J. Damage index based on stiffness degradation of low-rise RC walls. *Earthq. Eng. Struct. Dyn.* **2015**, *44*, 831–848. [CrossRef]
10. Chang, C.-M.; Chou, J.-Y. Damage Detection of Seismically Excited Buildings Based on Prediction Errors. *J. Aerosp. Eng.* **2018**, *31*, 04018032. [CrossRef]
11. Matarazzo, T.J.; Kurata, M.; Nishino, H.; Nishino, H.; Suzuki, A. Post earthquake strength assessment of steel moment-resisting frame with multiple beam-column fractures using local monitoring data. *J. Struct. Eng.* **2018**, *144*, 04017217. [CrossRef]
12. Zhou, Y.; Zhang, D.; Huang, Z.; Li, D. Deformation Capacity and Performance-Based Seismic Design for Reinforced Concrete Shear Walls. *J. Asian Arch. Build. Eng.* **2014**, *13*, 209–215. [CrossRef]
13. Belejo, A.; Barbosa, A.R.; Bento, R. Influence of ground motion duration on damage index-based fragility assessment of a plan-asymmetric non-ductile reinforced concrete building. *Eng. Struct.* **2017**, *151*, 682–703. [CrossRef]
14. Sun, P.; Zhai, C.; Wen, W. Experimental investigation on the damage accumulation of reinforced concrete columns under mainshock-aftershock sequences. *Earthq. Eng. Struct. Dyn.* **2021**, *50*, 4142–4160. [CrossRef]
15. Liu, Z.; Wang, Y.; Cao, Z.; Chen, Y.; Hu, Y. Seismic energy dissipation under variable amplitude loading for rectangular RC members in flexure. *Earthq. Eng. Struct. Dyn.* **2018**, *47*, 831–853. [CrossRef]
16. Fairhurst, M.; Bebamzadeh, A.; Ventura, C.E. Effect of Ground Motion Duration on Reinforced Concrete Shear Wall Buildings. *Earthq. Spectra* **2019**, *35*, 311–331. [CrossRef]
17. Park, Y.J.; Ang, H.S. Mechanistic seismic damage model for reinforced concrete. *J. Struct. Eng.* **1985**, *111*, 722–739. [CrossRef]
18. Park, Y.J.; Ang, H.S.; Wen, Y.K. Seismic damage analysis of reinforced concrete buildings. *J. Struct. Eng.* **1985**, *111*, 740–757. [CrossRef]
19. Syntzirma, D.V.; Pantazopoulou, S.J.; Aschheim, M. Load-History Effects on Deformation Capacity of Flexural Members Limited by Bar Buckling. *Eng. Struct.* **2010**, *136*, 1–11. [CrossRef]
20. Jason, C.; Mervyn, J.; James, M. Effect of load history on performance limit states of circular bridge columns. *J. Bridge Eng.* **2013**, *18*, 1383–1396.
21. Feng, Y.; Kowalsky, M.J.; Nau, J.M. Effect of Seismic Load History on Deformation Limit States for Longitudinal Bar Buckling in RC Circular Columns. *Eng. Struct.* **2015**, *141*, 04014187. [CrossRef]
22. Wang, Y.; Liu, Z.; Yang, W.; Hu, Y.; Chen, Y. Damage index of reinforced concrete members based on the energy dissipation capability degradation. *Struct. Des. Tall Spéc. Build.* **2020**, *29*, e1695. [CrossRef]
23. Kunnath, S.K.; Chai, Y.H. Cumulative damage-based inelastic cyclic demand spectrum. *Earthq. Eng. Struct. Dyn.* **2003**, *33*, 499–520. [CrossRef]
24. Miao, Z.W.; Ma, Q.L.; Ye, L.P. Study on energy based seismic design method of reinforced concrete frame structures. *J. Build. Struct.* **2013**, *34*, 1–10.
25. Arroyo, D.; Ordaz, M. On the estimation of hysteretic energy demands for SDOF systems. *Earthq. Eng. Struct. Dyn.* **2007**, *36*, 2365–2382. [CrossRef]
26. Chai, Y.H.; Fajfar, P.; Romstad, K.M. Formulation of Duration-Dependent Inelastic Seismic Design Spectrum. *Eng. Struct.* **1998**, *124*, 913–921. [CrossRef]
27. National Standard Seismic Code Management Group. *GB 50011-2010 Code for Seismic Design of Buildings*; China Architecture & Building Press: Beijing, China, 2016.

28. Liu, Z.F.; Wang, Y.K.; Cao, Z.X.; Chen, Y.P. Study on performance index of RC members considering effect of seismic duration. *J. Build. Struct.* **2018**, *39*, 168–177.
29. Wang, Y.; Liu, Z.; Zhang, D.; Hu, Z.; Yu, D. Seismic design of rectangular/square columns in SDOF systems based on their damage performance. *Sci. Prog.* **2022**, *105*, 00368504221127788. [CrossRef]